A Super-Earth caught in a trap

E. Podlewska* and E. Szuszkiewicz†

Institute of Physics and CASA*, University of Szczecin, ul. Wielkopolska 15, 70-451 Szczecin, Poland

ABSTRACT

This paper is an extension of the work done by Pierens & Nelson (2008) in which they have investigated the behaviour of a two-planet system embedded in a protoplanetary disc. They have put a Jupiter mass gas giant on the internal orbit and a lower mass planet on the external one. We consider here a similar problem taking into account a gas giant with masses in the range of 0.5 to $1M_J$ and a Super-Earth (i.e. a planet with mass $\leq 10 M_{\oplus}$) as the outermost planet. By changing disc parameters and planet masses we have succeeded in getting the convergent migration of the planets which allows for the possibility of their resonant locking. However, in the case in which the gas giant has the mass of Jupiter, before any mean motion first order commensurability could be achieved, the Super-Earth is caught in a trap when it is very close to the edge of the gap opened by the giant planet. This confirms the result obtained by Pierens & Nelson (2008) in their simulations. Additionally, we have found that, in a very thin disc, an apsidal resonance is observed in the system if the Super-Earth is captured in the trap. Moreover, the eccentricity of the small planet remains low, while the eccentricity of the gas giant increases slightly due to the imbalance between Lindblad and corotational resonances. We have also extended the work of Pierens & Nelson (2008) by studying analogous systems in which the gas giant is allowed to take Sub-Jupiter masses. In this case, after performing an extensive survey over all possible parameters, we have succeeded in getting the 1:2 mean motion resonant configuration only in a disc with low aspect ratio and low surface density. However, the resonance is maintained just for few thousand orbits. Thus, we conclude that for typical protoplanetary discs the mean motion commensurabilities are rare if the Super-Earth is located on the external orbit relative to the gas giant.

Key words: methods: numerical - planets and satellites: formation

INTRODUCTION

Among over 300 extrasolar planets discovered so far only a few Super-Earths, that is planets with masses in the range of 2-10 M_{\oplus} , have been observed. However, more candidates are just waiting to be confirmed and new discoveries are going to be announced, so we can soon find ourselves in the middle of the Super-Earth epoch. Some of such low-mass planets might exist in the neighborhood of gas giants and by means of numerical simulations it is possible to predict what are the most common configurations of extrasolar systems with Super-Earths and what will be detected by present and future observational programmes. It is believed that the observed architecture of the planetary systems might be an outcome of the large scale orbital migration induced by the disc-planet interactions. Depending on the planet masses and on the disc properties, two main regimes of orbital migration can be distinguished (Ward 1997).

† E-mail: szusz@univ.szczecin.pl (ES)

The migration time for low-mass planets or planetary embryos embedded in a gaseous disc has been derived first by summing the differential torques induced by the Lindblad resonances (Goldreich & Tremaine 1979; Ward 1997) and improved later by taking into account the contribution from the corotation torque (Tanaka et al. 2002)

$$\tau_I = (2.7 + 1.1\gamma)^{-1} \frac{M_*}{m_p} \frac{M_*}{\sum r_p^2} \left(\frac{c}{r_p \Omega_p}\right)^2 \Omega_p^{-1}$$
 (1)

Here m_p is mass of the planet, r_p is the distance from the central star M_* , Σ is the disc surface density, c and Ω_p are respectively the local sound speed and the angular velocity. The coefficient γ depends on the disc surface density profile, which is expressed as $\Sigma(r) \propto r^{-\gamma}$. Eq. (1) refers to type I migration, where the disc response is linear and the planet is not massive enough to perturb significantly the mass distribution of the gas in the disc. However, recent studies showed a strong departure from the linear theory. It has been found that in non-isothermal discs with high opacity (Paardekooper & Mellema 2006) in the presence of

^{*} E-mail: edvtap@univ.szczecin.pl (EP)

an entropy gradient (Paardekooper & Papaloizou 2008) the sign of the total torque can change reversing in this way the direction of the migration.

For high-mass planets the disc response becomes non linear and a gap forms in the disc around the planet orbit. If the gap is very clean and the disc is stationary, the evolution of the planet is determined by the radial velocity drift in the disc (Lin & Papaloizou 1986), namely

$$v_r = \frac{3\nu}{2r_p}. (2)$$

The migration time of the planet can be estimated as (Lin & Papaloizou 1993)

$$\tau_{II} = \frac{2r_p^2}{3\nu}.\tag{3}$$

However, recent numerical simulations (Edgar 2007) showed that the migration rate depends also on the planet mass and on the disc surface density profile, which can be written as

$$\tau_{II} = \frac{m_p}{3\nu\Sigma(r)}. (4)$$

The latter estimation gives a dependence on the surface density which is in good agreement with hydrodynamic simulations, although the variation with the disc viscosity appears to be much weaker than expected from analytical predictions (Edgar 2007, 2008).

For intermediate-mass planets which open the gap only partially, type III migration has been proposed (Masset & Papaloizou 2003). This type of migration occurs if the disc mass is much higher than the mass of the planet.

It is than required to employ numerical simulations in order to determine how the relative migration rate of the planets varies in details with their masses and with the parameters specifying the properties of the disc.

Different rates of planetary migration can lead to the resonant capture of the planets as it was shown for two giant planets in Kley (2000) or Kley, Peitz & Bryden (2004). Also low-mass planets may undergo convergent migration and form a resonant structure (Papaloizou & Szuszkiewicz 2005). In a previous paper of ours (Podlewska & Szuszkiewicz 2008), we have considered a system with low- and high-mass planets (a Super-Earth on the internal orbit and a Jupiter-like planet on the external one) and we have found that they are captured into 3:2 or 4:3 mean motion resonances if the disc properties allow for convergent migration. Without drawing a too close analogy to the formation of the Solar System. it has been pointed out that the Hilda and Thule groups of asteroids are in the interior 3:2 and 4:3 resonances with Jupiter. Similar configurations with a Super-Earth instead of an asteroid might be present in extrasolar planetary systems. In order to draw such a conclusion, a long-term stability analysis of the obtained resonant structures should be performed.

In the present work we examine a slightly different situation. As in Podlewska & Szuszkiewicz (2008) planets form a close pair and are embedded in the gaseous disc, but this time the Super-Earth lies on the external orbit. This case has been already studied by Thommes (2005) and more recently by Pierens & Nelson (2008) (hereafter PN08). Thommes (2005) has found that a Jupiter mass planet can act, at least for a certain time, as a safety net for low-mass

planets, capturing them into orbital commensurabilities. In his calculations, the low-mass planet, which is allowed to accrete the mass, migrates towards the Jupiter and ends up in a 1:2 or 2:3 resonance depending on the surface density of the disc. Contrary to his result, PN08 have noticed that a low-mass planet (in the range of 3.5 - 20 M_{\oplus}) can be trapped at the outer edge of the gap opened by the gas giant. Planets cannot therefore get close enough as it is necessary to attain a mean motion resonance. Such planet trapping mechanism is possible at the steep and positive surface density gradient in the radial profile of the gaseous disc where, the corotation torque compensates the differential Lindblad torque (Masset et al 2006). More recently Paardekooper & Papaloizou (2009) have studied the nonlinear effects arising in the coorbital region of planets of a few Earth masses. They have found that any positive density gradient in the disc can act as a protoplanetary trap.

The investigations of Thommes (2005) have been performed using a hybrid code, that combines an N-body component with a one-dimensional viscous disc model. In this way the effects of Lindblad torques are well reproduced, but the corotation torques acting on the low-mass planet are not taken into account. Employing a 2D hydrodynamical code, PN08 have been able to include properly both types of torques. It has been shown by PN08 that the initially convergent migration of a Jupiter mass gas giant and an outer planet less massive than 20 M_{\oplus} stops when the low-mass planet approaches the outer edge of the gap formed by the gas giant. Later on, the low-mass planets migrate outward. In the present work we confirm the results of PN08 in the case of a Super-Earth and a Jupiter-like planet. The only difference is that in the calculations of PN08 the low-mass planet was able to accrete matter from the disc and if its mass exceeded the value of 20 M_{\oplus} , the planets ended up in a mean-motion resonance. In this paper we are interested in Super-Earths, so we did not take into account accretion.

As an extension of the work of PN08, we have investigated the evolution of a Super-Earth also in the presence of Sub-Jupiter gas giants, whose masses are lower than that of Jupiter. For typical disc properties the gap opened by the gas giant is very wide and the positions of all first order mean motion commensurabilities are located inside the region affected by the gap. If the gas giant is assumed to be less massive than Jupiter (e.g. $0.5M_J$), the gap opened by the planet is narrower, which gives a chance for attaining a first order mean motion resonance. However, in this situation the migration of the gas giant is faster than that of the low-mass planet causing the divergent relative motion of both planets. For this reason, in order to get the commensurability one needs to slow down the Sub-Jupiter or to speed up the Super-Earth. Finally, we have achieved the 1:2 mean motion resonance for very thin discs and low surface density. This configuration, however, has not been maintained till the end of the simulations.

This paper is organized as follows. In Section 2 we describe our numerical set-up. In Section 3 we present the procedure used in order to achieve the convergent migration of a Super-Earth and a Jupiter-like planet. Section 4 is dedicated to the results obtained in the evolution of such a system of planets. We also discuss in this Section the eccentricity behaviour together with the analysis of the sensitivity of our results to numerical parameters and the occurrence of the

apsidal resonance. In Section 5 we investigate the scenario in which the Jupiter-like planet is substituted by a gas giant with a smaller mass. Finally, we summarize and discuss our findings in Section 6.

2 DESCRIPTION OF THE NUMERICAL SIMULATIONS

We have performed numerical simulations of a system containing two interacting planets and a gaseous protoplanetary disc with which the planets interact. One of the planets is a Super-Earth and the other is a gas giant. They are considered as point masses orbiting around the central star with mass $M_* = M_{\odot}$. The disc undergoes near-Keplerian rotation and its vertical semi-thickness H is small in comparison with the distance r from the central star. We assume a constant aspect ratio h = H/r, so that the temperature profile of the disc is $T \propto r^{-1}$. The best choice of coordinates for this problem is that of cylindrical coordinates (r, φ , z) with the origin located at the position of the central star. The equations of motion can be vertically averaged. In this way the problem is reduced to two dimensions, given by the radial and azimuthal directions. The evolution of the gaseous disc in our system is governed by the continuity equation and two equations of motion (for the full formulation, see Nelson et al. (2000)). We are not solving the full energy equation because of the high computational cost. The locally isothermal equation of state of the gas in the disc is adopted instead. However, it has been noticed that solving the energy equation could have dramatic effects on the migration of the low-mass planet (Paardekooper & Mellema 2006). Namely, in non-isothermal discs the migration can be directed outward. We have used the same Eulerian hydrodynamic code NIRVANA (Ziegler 1998) as in our previous paper (Podlewska & Szuszkiewicz 2008). The details of the numerical scheme can be found in Nelson et al. (2000). We have checked that the results obtained with our version of the NIRVANA code are in very good agreement with those obtained in the framework of the project "The Origin of Planetary Systems" (De Val-Borro et al. 2006). Following a common practice, in order to assess the robustness of our results we have repeated part of our investigation with a second code, which in our case was FARGO (Masset 2000). The initial surface density profile of the disc $\Sigma(r)$ is taken to be flat at the planet location. Its overall shape shown in (Fig. 1) has been constructed for computational convenience, namely to avoid an unwanted behaviour of the disc at the boundaries of the computational domain.

The surface density value $\Sigma_0=6\times 10^{-4}\left(\frac{M_\odot}{(5.2AU)^2}\right)$ of the flat part of this profile corresponds to the minimum mass solar nebula (MMSN) which consists of a gas weighing two Jupiter masses spread out within a circular area of radius equal to the mean distance of Jupiter from the Sun. The adopted unit of length corresponds to 5.2AU. The unit of time is given by $(GM_*/r_p^3)^{-1/2}$ (G is the gravitational constant, M_* denotes the mass of the star and r_p the initial radial position of the inner planet). This quantity amounts to $(1/2\pi)$ times the orbital period of the initial orbit of the inner planet and it will be called just an "orbit" throughout the whole paper. The initial locations of the planets and

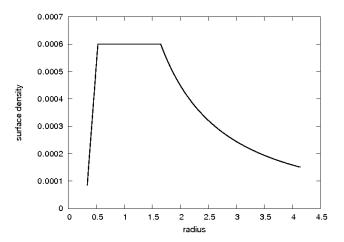


Figure 1. The initial surface density profile of the disc. The planets were initially located in the flat part of this profile.

their masses are given in Table 1. At the beginning of all runs we have put both planets on circular orbits in the flat part of the surface density profile. The computational domain extends between $r_{min} = 0.33$ and $r_{max} = 4.15$ in the radial direction as it is shown in Fig. 1. We have also performed one run with $r_{max} = 5$ in order to check the evolution for a larger initial separation of the planets. The azimuthal angle φ takes its values in the interval $[0, 2\pi]$. The disc is divided into 400×512 grid cells in the radial and azimuthal directions respectively. For the model with $r_{max} = 5$ we increased the resolution in such a way that the size of each single grid cell remains unchanged. We have also run one simulation with a higher number of grid cells (576×986) and we have found no significant difference in the migration rate and the eccentricity evolution, so we assume that our standard resolution is appropriate for our experiments. The radial boundary conditions were taken to be open, so that the material in the disc can outflow through the boundaries of the computational domain. In this case the profile of the disc changes with time. In order to avoid unrealistic effects due to gas depletion, we have run our simulations for no longer than 10⁴ orbits. The potential is softened with softening parameter $\varepsilon = 0.8H$. Some of the simulations have been run also with $\varepsilon = 0.6H$ and $\varepsilon = 1.3H$ in order to check the influence of the softening length on the evolution of the planets. In the calculation of the gravitational potential of the planets we do not exclude the matter contained in the planet Hill sphere. The selfgravity of the disc is not taken into account. In order to get the convergent migration of the planets when the gas giant is on the internal orbit and the Super-Earth on the external one, we have performed a series of numerical simulations using different disc parameters. All simulations are summarized in Table 1. We have run our experiments with constant aspect ratio h ranging from 0.03 to 0.05 and constant kinematic viscosity $\nu = 2 \cdot 10^{-6}$ in dimensionless units (this corresponds to the α parameter being equal to $2.2 \cdot 10^{-3}$ for h = 0.03 and $8 \cdot 10^{-4}$ for h = 0.05). In one case, a higher viscosity value ($\nu = 5 \cdot 10^{-6}$) has been used in order to obtain that the gap opened by the gas giant is very narrow. The last column in Table 1 shows whether we have achieved convergent migration or not. In this table

Table 1. In this table we summarize all the performed simulations. The first column shows the model number, the second the initial semi-major axis of the Jupiter, the third the initial semi-major axis of the Super-Earth, the fourth the outer edge of the disc, the fifth the mass of the Super-Earth, the sixth the mass of the gas giant, the seventh the surface density, the eighth the aspect ratio, the ninth the kinematic viscosity and the tenth the kind of relative migration of the planets. The comment "convergent/divergent" means that relative migration of the planets reversed during the evolution.

model	r_{p1}	r_{p2}	r_{max}	mass of the Super-Earth (M_{\oplus})	mass of the gas giant (M_J)	surface density	h	ν	migration
1	1	1.62	4.15	5.5	1	Σ_0	0.05	$5 \cdot 10^{-6}$	divergent
2	1	1.62	4.15	5.5	1	Σ_0	0.05	$2 \cdot 10^{-6}$	divergent
3	1	1.35	4.15	5.5	1	Σ_0	0.03	$2 \cdot 10^{-6}$	convergent/divergent
4	1	1.62	4.15	5.5	1	Σ_0	0.03	$2 \cdot 10^{-6}$	convergent/divergent
5	1	1.58	4.15	5.5	1	Σ_0	0.03	$2 \cdot 10^{-6}$	convergent/divergent
6	1	2.2	5	5.5	1	Σ_0	0.03	$2 \cdot 10^{-6}$	convergent/divergent
7	1	1.62	4.15	5.5	1	$2\Sigma_0$	0.05	$2 \cdot 10^{-6}$	convergent/divergent
8	1	1.62	4.15	10	0.5	$1.5\Sigma_0$	0.05	$2 \cdot 10^{-6}$	divergent
9	1	1.62	4.15	10	0.5	$2.5\Sigma_0$	0.05	$2 \cdot 10^{-6}$	divergent
10	1	1.62	4.15	10	0.6	$1.5\Sigma_0$	0.05	$2 \cdot 10^{-6}$	divergent
11	1	1.62	4.15	10	0.7	$1.5\Sigma_0$	0.05	$2 \cdot 10^{-6}$	divergent
12	1	1.62	4.15	10	0.5	Σ_0	0.03	$2 \cdot 10^{-6}$	convergent/divergent
13	1	1.62	4.15	10	0.5	Σ_0	0.04	$2 \cdot 10^{-6}$	convergent/divergent
14	1	1.62	4.15	10	0.5	$0.5\Sigma_0$	0.03	$2 \cdot 10^{-6}$	convergent

[&]quot;convergent/divergent" means that the relative migration of the planets reversed during the evolution.

3 LOOKING FOR THE CONVERGENT MIGRATION OF A SUPER-EARTH AND A JUPITER

Similarly as in our previous paper, we have tried to determine the initial conditions appropriate for the convergent migration using the analytic formulae given by equations (1) for the Super-Earth and (3) or (4) for the gas giant. However, we have found as in Edgar (2007) that in an isothermal viscous disc a giant planet does not obey the standard type II migration and hence migration does not proceed on the viscous timescale. That is why we have performed a series of numerical experiments in order to examine under which conditions it is possible to obtain convergent migration.

Using the full 2D hydrodynamical code NIRVANA we have calculated the evolution of the orbital elements of the planets embedded in the gaseous disc in the region where the exterior first order mean motion resonances are located. The gas giant planet has been placed always at the distance 1 in our units and the Super-Earth further away from the star (see Table 1), starting from a small separation between planets of the order of a few Jupiter's Hill radii, and then increasing it. Planets are not allowed to accrete matter and their masses are fixed for the whole time of the calculations.

We have analyzed different disc models changing the aspect ratio, the kinematic viscosity and the surface density of the disc. These investigations allowed us to find the condi-

tions under which the migration is convergent at the beginning of the evolution. This does not imply that it will remain convergent throughout the whole run. In fact, in most of our models divergent migration is the final outcome. If the kinematic viscosity is high, for instance $\nu = 5 \cdot 10^{-6}$ (h = 0.05and $\Sigma = \Sigma_0$), the migration of the Jupiter is fast and the relative migration of both planets is divergent (Table 1, model 1). For gas giants the migration speed is evaluated to be proportional to the viscosity of the disc (Lin & Papaloizou 1993), so if we take a lower value of ν , the migration of the Jupiter is slower. Assuming for the kinematic viscosity the value $\nu = 2 \cdot 10^{-6}$ without changing other parameters (Table 1, model 2), we have obtained indeed a slower migration than in model 1 as it is shown in Fig. 2, but still the relative motion of both planets is divergent. We have noted that the migration of the gas giant is faster than that of the Super-Earth even after pushing the kinematic viscosity as low as $\nu = 8 \cdot 10^{-7}$. We conclude that convergent migration cannot be achieved changing only the viscosity of the disc. It was shown by (Edgar 2007) that the migration of the gas giant depends also on the surface density, so we have continued our search for convergent migration changing other disc properties. A full analysis of the influence of the disc parameters on the gap profile and thus on the migration of the planet can be found in Crida et al. (2006). We have performed simulations with relatively low ν (2·10⁻⁶) changing h and Σ . First, we have set $\Sigma = \Sigma_0$ and achieved the convergent migration of both planets for a very thin disc with aspect ratio h = 0.03 (for example model 4). In this case, the gap opened by the gas giant is very wide and the migration of the Jupiter is slower than that of the Super-

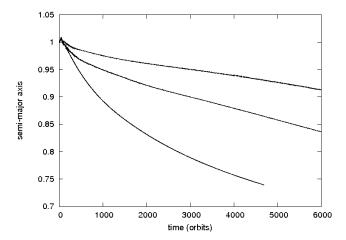


Figure 2. The semi-major axis of the Jupiter for models 1 (lowest curve), model 2 (middle curve) and model 3 (upper curve) of Table 1.

Earth, which causes that the radial distance between the planets decreases. Convergent migration has been obtained also keeping the aspect ratio fixed (h=0.05) and changing the surface density. Taking $\Sigma=2\Sigma_0$, (as in model 7) we have got a migration of the Super-Earth which is faster than in model 2 in accordance to the simple approximation of type I migration (Tanaka et al. 2002) and at the same time the migration is convergent.

4 THE EVOLUTION OF THE SUPER-EARTH AND THE JUPITER

4.1 The semi-major axis evolution

In PN08 it has been discussed the evolution of a two-planet system containing a low-mass planet with a mass in the range of $3.5-20M_{\oplus}$ and a Jupiter mass planet, both embedded in a disc with the surface density $\Sigma \propto r^{-3/2}$. According to PN08 this evolution should end up with the trapping of the low-mass planet near the outer edge of the gap produced by the Jupiter mass planet. In this Section we are interested in the possibility of resonant locking of a Super-Earth with mass $5.5M_{\oplus}$ and a Jupiter mass planet embedded in a disc with a flat surface density profile. In order to check whether the outcome of the evolution of the system considered here is the same as in PN08, we have performed a series of simulations which are described below.

In Fig. 3 we show the evolution of the semi-major axis ratio of the planets in the case where the initial planetary orbital separation is 0.35 (Table 1, model 3). The semi-major axis ratio has been calculated by dividing the semi-major axis of the Super-Earth by the semi-major axis of the gas giant. The convergent migration brings planets into the 2:3 mean motion commensurability. The horizontal lines in Fig. 3 show the width of this resonance (Lecar et al. 2001). However, this configuration lasts just for a few hundreds of orbits and after that the relative distance between the planets increases. The Super-Earth migrates outward and the Jupiter migrates inward, as expected, with a rate determined by its mass and by the disc parameters. It is then clear that the

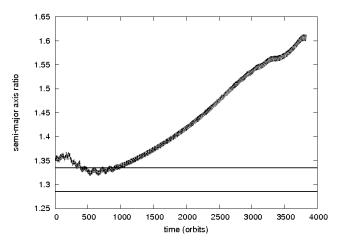


Figure 3. The semi-major axis ratio of the planets versus time. The initial planet separation is 0.35 (model 3 of Table 1). The planets have been captured in the 2:3 mean-motion resonance (exact position of the commensurability is 1.31) but the resonant structure did not last and the migration became divergent. The horizontal lines denote the width of the 2:3 commensurability.

evolution of the Super-Earth is responsible for reversing the convergent relative motion of the planets into a divergent one after roughly 1000 orbits.

Next, we have checked the possibility of the occurrence of the other first order commensurability found by Thommes (2005), namely 1:2. To this aim, we have placed the Super-Earth further out from the Jupiter, at the relative orbital separation of 0.62 (Table 1, model 4). The evolution of this configuration is shown in Fig. 4 (left panel). The convergent migration continues for about 2000 orbits and after that, similarly as in model 3, the Super-Earth migrates outward. In the right panel of Fig. 4 we have plotted again the behaviour of the Super-Earth, but this time using a different scale, in order to see its orbital evolution in full detail. In Fig. 5 we have illustrated the evolution of the ratio of the semi-major axes of the planets. This ratio lies outside the resonance region whose width is marked by two horizontal lines (Lecar et al. 2001). Next, we have put the planets exactly in the 1:2 resonance (Table 1, model 5) and we have obtained the same result seen in model 4. For a disc with higher surface density and aspect ratio h = 0.05 (as in the model 7), we have also obtained convergent migration at the beginning, but later on the relative migration of the planets reversed as in the previous models. As a result, no mean motion commensurability has been attained. Our conclusion is that even the most distant first order 1:2 mean motion resonance cannot be achieved in this way.

Similar results have been presented by PN08 in the case in which the outer planet has mass $10M_{\oplus}$ or $20M_{\oplus}$. The answer to the question why the Super-Earth is not able to form resonant configuration with the gas giant is illustrated in Fig. 6, where we show the surface density profile changes in model 4 after about 2355, 3925 and 7850 orbits, together with the position of the Super-Earth marked by black dots. It can be seen that the outer edge of the gap in moving slowly outward but the planet remains trapped in the high surface density region at the edge of the cavity till the end of

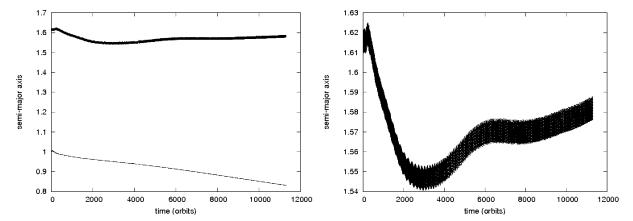


Figure 4. Left panel: The semi-major axis of planets with initial separation of 0.62 (model 4 of Table 1). The upper curve refers to the Super-Earth and the lower one to the gas giant. Right panel: The evolution of the semi-major axis of the Super-Earth for the same model, but with a different scale in the vertical axis. At the beginning the Super-Earth migrates inward but later on the migration has changed the direction because the planet is trapped and it moves together with the edge of the gap.

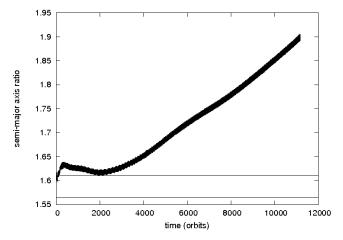


Figure 5. The semi-major axis ratio of the planets with the initial separation of 0.62 (model 4 of Table 1). The exact position of the resonance is 1.58. The migration becomes divergent before the planets could enter the resonant region denoted by the horizontal lines.

the simulation. The same situation was observed in PN08. However, in their paper the outer planet is more massive than in our simulations and it is stopped closer to the gas giant where the vortensity gradient is larger. From the analysis of the position of the Super-Earth relative to the gap, we conclude that the outward migration of this planet seen in Fig. 4 is caused by the evolution of the gap opened by the gas giant in the disc. So the migration of the two planets is convergent until the Super-Earth is trapped. After that, the migration reverses and the Super-Earth moves together with the expanding edge of the gap as reported in PN08.

The models discussed till now have one common feature, namely the planets are placed initially very close to the resonance (models 3, 4 and 7) or exactly in the resonance (model 5). This choice has been made for computational reasons. However, locating the planets far away from

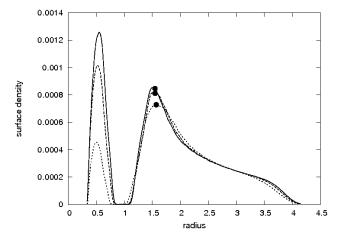


Figure 6. The surface density profile of the disc after 2355 (solid line), 3925 (dashed line) and 7850 (dotted line) orbits for model 4 of Table 1. The dots denote the positions of the Super-Earth.

the first order commensurabilities would be useful for the interpretation of our results. Having this in mind, we have performed also one experiment with a relatively large initial orbital separation between planets like in PN08 (Table 1, model 6). The outcome of the evolution of this model is that the Super-Earth is caught again in the trap at the edge of the gap.

In all the models where we have obtained convergent migration the gap is wide and the position of the 1:2 resonance is always inside the gap. This fact is illustrated in Fig. 7, where we plot the gap profile of the outer part of the disc for model 4 after 3925 orbits. The dots denote the position of the Super-Earth and of the Jupiter. The vertical line shows the location of the 1:2 commensurability. The Super-Earth is captured in the trap which prevents the further migration towards the resonance.

In order to avoid the process connected to the cavity

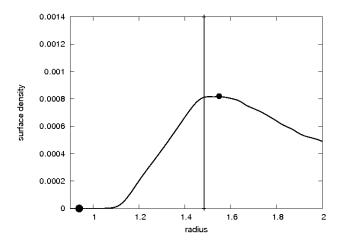


Figure 7. The surface density profile of the outer edge of the gap in the model 4 after 3925 orbits. The dots denote the positions of the planets, the vertical line the location of the 1:2 mean motion resonance. The Super-Earth is captured in the trap so it cannot approach the commensurability.

opening which can influence the disc structure in the vicinity of the gas giant, we have performed a simulation in which the Jupiter was initially located in a fully formed gap. We have used in this simulation a disc profile in which the shape of the gap has been obtained from that of model 4 after eliminating the bumps at the edges of the cavity. In this way the surface density maxima outside the edges, which are a consequence of the gap formation and could affect the results, are absent. Also in this case, the Super-Earth migrated slowly inward and was captured in the trap as in the previous models. The assumption of the existence of the initial gap enabled us to study the evolution in a more realistic way.

4.2 The eccentricity evolution

We investigated also the evolution of the eccentricities of the planets. At the beginning of our simulations both planets are located on circular orbits. First, let us have a look at the eccentricity of the Super-Earth. When the migration is convergent, the planets approach the 1:2 resonance and the Super-Earth's eccentricity increases slightly, see for instance Fig. 8, which describes the case of model 4 of Table 1. As soon as the Super-Earth is trapped at the edge of the gap, the planets depart from the resonance and the Super-Earth's eccentricity is damped by the tidal interaction with the disc to a low value and remains at this level till the end of the simulation. In case where the migration is always divergent since the beginning of the simulation, the eccentricity of the Super-Earth remains low during the whole time of the evolution.

As far as the gas giant is concerned, during its evolution in the disc the eccentricity is very low in most cases. However, we have found an interesting feature in the discs with aspect ratio h=0.03. Namely, the eccentricity increases for the first few thousand orbits, later on its growth is slowed down and at the end of the simulation approaches the value of 0.04-0.05. We have investigated this issue in detail and we have checked the dependence of the eccentricity growth

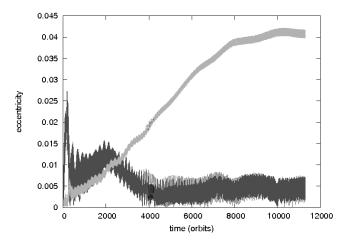


Figure 8. The eccentricity evolution of the gas giant (gray colour) and the Super-Earth (black colour) for model 4 of Table 1.

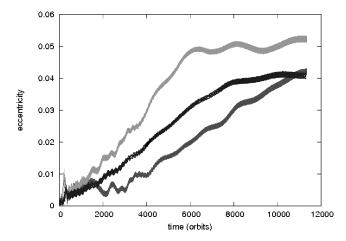


Figure 9. The eccentricity of the gas giant with $\varepsilon = 0.6H$ (light gray curve), $\varepsilon = 0.8H$ (dark gray curve) and $\varepsilon = 1.3H$ (black curve) for model 4 of Table 1. The eccentricity increased in all cases.

on numerical parameters such as the softening length and the grid resolution. We have performed simulations with the same set-up of model 4 using for the softening parameter the values $\varepsilon = 0.6H, \ \varepsilon = 0.8H$ and $\varepsilon = 1.3H,$ which correspond respectively to the following values of the radius of the Jupiter's Hill sphere: 0.26, 0.35 and 0.58. In Fig. 9 we compare the evolution of the eccentricity of the gas giant with these three parameters. Despite some differences at the initial stages of the evolution, the result is approximately the same in each simulation. It is important to mention at this point that the evolution of the gas giant eccentricity is the same in all calculated models with h = 0.03. In order to check the effects of the grid resolution we have repeated the run of model 4 with lower resolution (192 \times 256 grid cells in the radial and azimuthal direction respectively) and we didn't observe any eccentricity growth. This suggests that to detect this behaviour one needs higher grid resolutions. We have also run this simulation with a higher number of grid cells (576×986) and we have found no significant difference in the migration rate and the eccentricity evolution.

An extensive discussion is going on in the literature on the possible mechanisms for exciting eccentricities (e.g. Artymowicz et al. (1991),Papaloizou, Nelson & Masset Goldreich & Sari (2003)Ogilvie & Lubow (2001).(2003), Sari & Goldreich (2004), D'Angelo et al. (2006), Kley & Dirksen (2006)). This interest is driven by the observed properties of the known extrasolar systems. One possible origin of the non-zero eccentricities of extrasolar Jupiters is the planet-disc interaction, which is most relevant in our calculations. Goldreich & Sari (2003) and Sari & Goldreich (2004) have estimated that eccentric Lindblad resonances can cause the eccentricity growth if the planet can open a very clean gap in the disc. Papaloizou, Nelson & Masset (2001) have found that for standard disc parameters this mechanism of eccentricity growth can work for bodies on initially circular orbits if the mass of the body is larger than 10 Jupiter masses. However, they do not exclude the possibility that for different disc parameters the mass of the planet in question might be smaller. For our set of disc parameters (h = 0.03 and $\nu = 2 \cdot 10^{-6}$) the gap is wide enough and we can observe the eccentricity growth.

The outcome of the scenario studied here is that the Jupiter is on a slightly eccentric orbit and the Super-Earth is on an almost circular one. This fact has interesting consequences from the astrobiological point of view and we will come back to this issue in the last Section.

4.3 The apsidal resonance

Despite the absence of mean motion commensurabilities between the Super-Earth and the Jupiter mass planet we have found the apsidal resonance in models 3, 4 and 5. Both resonant angles circulate in the whole range between 0 and 2π . At the beginning of the evolution the angle between the apsidal lines of the planetary orbits spans the whole interval between 0 and 2π and then, when the Super-Earth is already captured in the trap, it starts to librate around the value of π with an amplitude of about 90°, as it has been illustrated in Fig. 10. This behaviour indicates that the system is in apsidal resonance and in antialigned configuration. A similar behaviour of the apsidal lines has been already observed in extrasolar planetary systems, for example in vAnd and 47UMa (Laughlin, Chambers & Fisher 2002; Barnes & Greenberg 2006a). It has been noticed (Barnes & Greenberg 2006a,b) that planetary systems, as for example vAnd and 47UMa, can display the secular behaviour close to the separatrix between libration and circulation. The eccentricity growth can lead to the passage from one mode of the secular behaviour to another. In our simulations the apsidal resonance occurs only in those models in which the Super-Earth is trapped and the eccentricity of the Jupiter increases. The eccentricity growth can be a promising mechanism for establishing the apsidal resonance. The full analysis of this issue requires simulations covering the long timescales which are characteristic for the secular evolution.

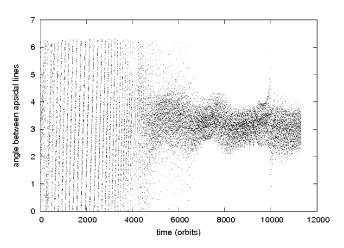
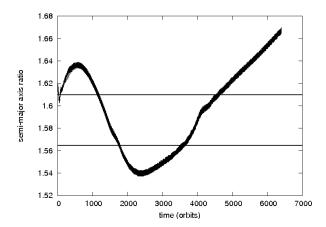


Figure 10. The evolution of the angle between the apsidal lines of the planetary orbits for model 4. After the capture of the planet in the apsidal resonance, the angle librates around π .

5 THE EVOLUTION OF THE SUPER-EARTH AND THE SUB-JUPITER

As we have shown in Section 4.1, the gap opened by the Jupiter mass planet is too wide to attain any first order mean motion commensurability, so we have checked if resonances are possible for Sub-Jupiter mass planets where the gap is narrower and the 1:2 resonance is located outside the gap. In this way there is a chance that the Super-Earth is captured into this commensurability before reaching the outer edge of the gap where it can be trapped. We have tried the cases, in which the masses of the Sub-Jupiters are 0.7, 0.6 and 0.5 M_{J} . For the 0.7 M_J case (model 11) the gap is still too wide and the position of the 1:2 resonance is still inside it. In the two other cases the gap widths allow the possibility of resonant locking. If the mass of the gas giant decreases, its migration rate increases, because such migrators cannot entirely open the gap and experience an additional torque which pushes them faster toward the star (Edgar 2007). This means that it is more difficult to get convergent migration in the case of Sub-Jupiters. On the contrary, for low-mass planets the migration rate increases with increasing mass of the planet. For this reason, in this Section we have taken the mass of the Super-Earth to be equal to $10M_{\oplus}$, instead of $5.5M_{\oplus}$, in order to get the fastest possible migration for the Super-Earth. In a first set of experiments we have chosen for the kinematic viscosity the value $\nu = 2 \cdot 10^{-6}$ and for the aspect ratio the typical value h = 0.05. The parameter which has been allowed to vary in order to obtain convergent migration is the surface density Σ . Let us note that for Σ higher than $2\Sigma_0$ we enter into the regime of the runaway type III migration of the gas giant (Masset & Papaloizou 2003). In this case the Sub-Jupiter migrates very fast and reaches the inner part of the disc after just a few hundreds of orbits. In discs with lower surface densities the migration was always divergent. In a second run of experiments, we have fixed the surface density to be $\Sigma = \Sigma_0$ trying instead different aspect ratios. For the Sub-Jupiter gas giant we have managed to achieve the convergent migration of the planets for h = 0.03 (model 12). For this choice of parameters, the relative migration of the planets is too fast and they passed through the 1:2 mean



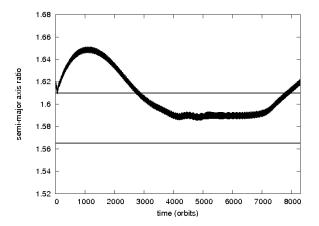


Figure 11. The semi-major axis ratio of the planets for model 12 (left panel) and model 14 (right panel). The horizontal lines denote the width of the 1:2 mean motion resonance.

motion resonance without being captured into this commensurability. They migrated further until the Super-Earth was trapped at the edge of the gap after 2400 orbits. Successively the migration reversed as it is shown in Fig. 11 (left panel) and the planets passed again through the resonance region without being captured. In order to slow down the relative radial motion of the planets, we have assumed in model 13 the higher aspect ratio of the disc h=0.04, without changing other parameters. In this case, the relative migration of the planets at the beginning was slowly convergent but later on became divergent.

Finally, we have achieved the 1:2 mean motion resonance for a disc with h = 0.03, $\nu = 2 \cdot 10^{-6}$ and $\Sigma = 0.5\Sigma_0$ (model 14). The lower surface density causes a slower migration of the Super-Earth and the convergent relative migration of the planets was slower than in model 12. In Fig. 11 (right panel) we present the semi-major axis ratio of the planets. The divergent migration during the first 1000 orbits is caused by the gas giant during the gap opening process. It can be seen that after 3000 orbits the planets approach the commensurability, both resonant angles and the angle between apsidal lines starts to librate around π and the eccentricities of the planets increase. However, at the end, the planets migrate out of the resonance. The Super-Earth with mass of 10 M_{\oplus} opens a shallow dip, which moves along with the migrating planet. The superposition of the dip and the outer edge of the gap creates a trap and leads to the capture of the Super-Earth.

From the above investigations we conclude that mean motion resonances between a gas giant and a Super-Earth which is located further away in the disc should be rare. If the mass of the gas giant is higher than $0.7M_J$, the gap opened by the planet is wide and the Super-Earth is captured in the trap before reaching the mean motion commensurability. For lower mass gas giants the gap is narrower and allows in principle the occurrence of the 1:2 resonance, but the migration of the gas giant is too fast for that. Our analysis, in which different disc parameters have been examined, shows that it is possible to obtain the short-lasting 1:2 mean motion commensurability between a Sub-Jupiter mass gas giant on the internal orbit and a Super-Earth on

the external one only for very thin discs with low surface density.

6 DISCUSSION AND CONCLUSIONS

The large-scale orbital migration in young planetary systems might play an important role in shaping up their architectures. The tidal gravitational forces are able to rearrange the planet positions according to their masses and disc parameters. The final configuration after the disc dispersal might be what we actually observe in extrasolar systems. In particular, in a system with a gas giant and a Super-Earth the convergent migration can lead to mean motion resonant locking or the Super-Earth is captured at the outer edge of the gap. The final outcome depends on the masses of the planets and on the disc parameters. We have investigated the evolution of the Super-Earth and of the gas giant embedded in a gaseous disc when the Super-Earth is on the external orbit and the gas giant on the internal one similarly as in PN08. However, we have concentrated here on systems with outer planet no more massive than $10M_{\oplus}$ and we have explored in details the evolution of such systems extending in this way the investigations done in PN08. We have changed the initial radial location of the Super-Earth, the masses of the planets and the disc parameters in order to check the possibility of locking into the 2:3 and 1:2 commensurabilities. What we have found is that it is difficult to obtain mean motion resonant configurations between planets. For the set of disc parameters and planet masses considered in this paper, it turns out that either the migration is divergent, or the Super-Earth migrates faster than the Jupiter until it is trapped at the outer edge of the gap opened by the gas giant. Thus, the trapping of the Super-Earth at the edge of the gap prevents the capture in the mean motion resonance because the gap is too wide and the resonant region is inside it.

In our studies we have investigated the behaviour of a Super-Earth, which means a planet with a mass not bigger than $10M_{\oplus}$, in the presence of a gas giant. Switching on the accretion, would result in exceeding the mass limit for a Super-Earth, so we didn't take accretion into account. How-

ever, if we allow the planets to accrete the matter than the planet is released from the trap and it forms the resonant structure, as it has been shown in PN08.

If the mass of the gas giant is low enough the gap is narrow and the 1:2 mean motion resonance is allowed. For a system with a Sub-Jupiter mass planet on the internal orbit and a Super-Earth on the external one, we have observed the resonant configuration only for very thin discs with low surface density. The resonant configuration did not hold during the evolution, so no mean motion resonance has been observed at the end of our simulations. Moreover, for a gas giant planet with Jupiter mass we have obtained a configuration in which the apsidal resonance is present if the Super-Earth is captured at the edge of the gap. Similar structures between apsidal lines are actually observed in vAnd and 47UMa extrasolar planetary systems.

The disc properties used here have been determined by the requirement of convergent migration in the disc. In the relatively thin disc with aspect ratio h=0.03 (models 3-6) we have found that the eccentricity of the gas giant increases, while the eccentricity of the Super-Earth remains very low. The growth of the Jupiter eccentricity is modest but well pronounced.

The fact that the Super-Earth remains on an almost circular orbit can have important implications for the habitability of such planets. As an example, let us consider a system containing a gas giant inside the habitable zone. Then, small planets or planetary embryos can survive the evolution of the system being captured at the outer edge of the gap opened by the giant planet and thus can be located exactly in the habitable zone. One of the possible places to look for such configurations is the system HD 27442. Another interesting object is ρCrB , a star with a Jupiter-like planet which has the eccentricity equal to 0.04, like the system discussed in this paper. Future observations will be able to test the proposed scenario, showing the way in which planetary migration can shape the planetary orbits.

ACKNOWLEDGMENTS

This work has been partially supported by MNiSW grant N203 026 32/3831 (2007-2010) and MNiSW PMN grant - ASTROSIM-PL "Computational Astrophysics. The formation and evolution of structures in the universe: from planets to galaxies" (2008-2010). The simulations reported here were performed using the Polish National Cluster of Linux Systems (CLUSTERIX) and the HAL9000 cluster of the Faculty of Mathematics and Physics of the University of Szczecin. We wanted to thank the referee for valuable comments which helped to improve the manuscript. We are grateful to John Papaloizou for enlightening discussions. We wish also to thank Adam Lacny for his helpful discussions and comments. Finally, we are indebted to Franco Ferrari for his continuous support in the development of our computational techniques and computer facilities and for reading the manuscript.

REFERENCES

Artymowicz, P., Clarke, C. J., Lubow, S. H., & Pringle, J. E. 1991, ApJ, 370, L35

Barnes, R., Greenberg, R., 2006a, ApJ, 638, 478

Barnes, R., Greenberg, R., 2006b, ApJ, 652, L53

Bryden, G., Chen, X., Lin, D. N. C., Nelson, R.P., Papaloizou, J.C.B., 1999, ApJ, 514, 344

Crida, A.; Morbidelli, A.; Masset, F., 2006, Icarus, 181, 587
 D'Angelo. G., Lubow, S. H., Bate, M. R., 2006, ApJ, 652, 1698

De Val-Borro, M., Edgar, R. G. Artymowicz, P. and 20 coauthors 2006, MNRAS, 370, 529

Edgar, R. G., 2007, ApJ, 663, 1325

Edgar, R. G., 2008, arXiv:0807.0625

Gladman, B, 1993, Icarus, 106, 247

Goldreich, P., & Tremaine, S., 1979, ApJ, 233, 857

Goldreich, P., & Sari, R., 2003, ApJ, 585, 1024

Ida, S., Lin, D. N. C., 2004, ApJ, 604, 388

Kley, W., 2000, MNRAS, 313, L47

Kley, W.; Peitz, J.; Bryden, G., 2004, A&A, 414, 735

Kley, W., Dirksen, G., 2006, A&A, 447, 369

Laughlin, G., Chambers, J., Fischer, D., 2002, ApJ, 579, 455

Lecar, M., Franklin, F. A., Holman, M. J., Murray, N. J., 2001. ARA&A 39, 581

Lin, D. N. C., Papaloizou, J. C. B., 1986, ApJ, 309, 846

Lin, D. N. C., Papaloizou, J. C. B., 1993, Protostars and planets III, 749

Masset, F. S., 2000, A&AS, 141, 165

Masset, F. S., Morbidelli, A., Crida, A., Ferreira, J., 2006, ApJ, 642, 478

Masset, F. S., Papaloizou, J. C. B., 2003, ApJ, 588, 494
Nelson R. P., Papaloizou J.C. B., Masset F., Kley W., 2000, MNRAS, 318, 18

Ogilvie, G. I., & Lubow, S. H. 2003, ApJ, 587, 398

Paardekooper, S.-J.; Mellema, G., 2006, A&A, 459, L17Paardekooper, S.-J., & Papaloizou, J. C. B., 2008, A&A, 485, 877

Paardekooper, S.-J., & Papaloizou, J. C. B., 2009, MNRAS, 394, 2283

Papaloizou, J. C. B., Nelson, R. P., & Masset, F. 2001, A&A, 366, 263

Papaloizou, J. C. B., Szuszkiewicz, E., 2005, MNRAS, 363, $153\,$

Pierens, A., Nelson, R. P., 2008, A&A, 482, 333

Podlewska, E., Szuszkiewicz, E., 2008, MNRAS, 386,1347

Sari, R. & Goldreich, P. 2004, ApJ, 606, L77

Tanaka, H., Takeuchi, T., Ward, W. R., 2002, ApJ, 565, 1257

Thommes, E. W., 2005, ApJ, 626, 1033

Ward, W. R., 1997, Icarus, 126, 261

Zhou, J.-L, Sun, Y.-S., 2003, ApJ, 598, 1290

Ziegler, U., 1998, Comp. Phys. Comm., 109, 111